Journal of Microscopy, Vol. 229, Pt 2 2008, pp. 377–383
Received 28 September 2006; accepted 20 May 2007

Polarization-maintaining near-field optical probes

S. PATANÈ*, E. CEFALÌ*, S. SPADARO*, R. GARDELLI*,
M. ALBANI† & M. ALLEGRINI‡
**Dipartimento di Fisica della Materia e Tecnologie Fisiche Avanzate, Università di Messina, Salita Sperone 31, I-98166 Messina, Italy*
†Dipartimento Ingegneria dell'Informazione. Università di Siena, Via Roma 56, 53100 Siena, Italy
‡Dipartimento di Fisica 'Enrico Fermi', Università di Pisa, and polyLAB-CNR, Largo Bruno Pontecorvo 3, I-56127 Pisa, Italy

Key words. Aperture near-field probes, near-field polarization, scanning near-field optical microscopy.

Summary

We demonstrate that tapered optical fibre probes can be easily modified in the taper cone to realize an electric dipole producing a well-defined near-field polarized light. This novel structure is made of a Short-cut Double C–shaped probe design combined to the usual full metal coating near the tapered end of the fibre. Hence, the cone at the apex of the probe is excited by an equivalent dipole whose spatial orientation is dictated by the probe geometry, regardless the polarization state of the incoming light. Properties and performances of such a configuration are first predicted by a finite-difference time domain simulation, showing that the near field coming out from the probe is linearly polarized. Following this novel design, a probe prototype is manufactured and tested. Its measured polar diagram confirms the polarization maintenance property in the near field.

Introduction

Scanning near-field optical microscopy (SNOM) is a surface technique providing optical images with spatial resolution beyond the diffraction limit (Lewis *et al.*, 1984; Pohl *et al.*, 1984). The probes are SNOM key components because the optical spatial resolution depends on the confinement of optical energy at the apex of the probe. Despite some drawbacks such as low throughput or tip heating effects, the most widely used near-field probes are tapered optical fibres. They consist of common optical fibres with one end tapered and metal coated in order to create a sub-wavelength aperture. The performances of near-field microscopes based on these tapered aperture probes are strongly related both to the aperture size and shape and to the taper geometry and structure. Light propagation and mode structure in these special waveguides are completely different from unperturbed fibres (Novotny & Hafner, 1994; Hecht *et al.*, 2000). Although these issues are nowadays quite well understood [for a comprehensive view see e.g. Novotny & Hecht (2006)], the polarization behaviour and control of SNOM tips is still difficult. Since the knowledge of the polarization is very important for the interpretation of SNOM images (Betzig *et al.*, 1992), great efforts have been made to elucidate this point, and two-dimensional (Novotny & Hafner, 1994) and three-dimensional (Huser *et al.*, 1999) models have been developed. The concept of degree of polarization for electromagnetic near fields (Setälä *et al.*, 2002a), including those of thermally fluctuating half-space sources (Setälä *et al.*, 2002b), has also been clarified. A well-defined and controlled polarization in near field is also important for applications such as polarimetry SNOM (Fasolka *et al.*, 2003), investigation of magneto-optical effects (Ono *et al.*, 2005), optical nanowriting on photosensitive polymers (Likodimos *et al.*, 2003), polarization-modulation SNOM where optical anisotropy associated with material structures and/or strain is measured (Lacoste *et al.*, 1998; Ramoino *et al.*, 2002; Ambrosio *et al.*, 2004). Polarization employed as contrast mechanism for SNOM imaging is also useful to distinguish between genuine optical effects and those arising from topographic artefacts (Valaskovic *et al.*, 1995). Specific work has been devoted to get a linear- or a circular-polarized near-field light coming out from SNOM aperture probes (Adelmann *et al.*, 1999; Shin *et al.*, 1999). The difficulties encountered to achieve a defined near-field polarization are mainly due to fibre birefringence and grain imperfections on the metal coating of the taper zone. At the fibre apex, the polarization is *not linear* because small tensions or torsions caused by even a slight fibre bending provoke strain-induced birefringence. Uncoated tapered fibres

Correspondence to: Dr Eugenio Cefalì, Tel +39 090 3977376; fax: +39 090 391382; e-mail: eugenio_cefali@ortica.unime.it

can overcome birefringence problems (Adelmann *et al.*, 1999), however, at the expense of spatial resolution. The metal coating process usually is not able to produce a grain-free nanoaperture with a perfect circular shape. Such defects induce highly asymmetric polarization behaviour of the near-field light coming out from the probe (Veerman *et al.*, 1998, 1999). A focussed ion beam (FIB) technique has been applied to 'clean' off the grainy coating metal at the end of the tip (Pilevar *et al.*, 1998; Veerman *et al.*, 1998, 1999). This technique produces a smooth and very flat-end face with a well-defined circularly symmetric aperture down to 20 nm that improves the polarization behaviour of the tip to polarization ratios exceeding 1:100 in all directions (Veerman *et al.*, 1998). Elliptical core fibres, coated with aluminium and with aperture milled by FIB, yield high throughput and are able to maintain the polarization (Adiga *et al.*, 2006). These results are satisfactory but the FIB technique is rather expensive and complex. Recently, a model for an SNOM probe incorporating metallic strips on the surface of a dielectric cone has been proposed (Lapchuk & Kryuchyn, 2004). This structure can be made by deposition of two metal strips instead of the full metal coating in the tapered zone of the fibre. It mimics an electric dipole able to efficiently drive a Quasi-TEM mode up to the end of the fibre. Unfortunately, the equivalent radiant dipole has a poor near field-to-far field ratio that does not allow practical applications as SNOM probe.

Based on the same electric dipole idea of reference (Lapchuk & Kryuchyn, 2004), in this work we demonstrate a new aperture probe design able to produce a well-defined polarized near field that does not depend on the polarization state of the light coupled into the fibre. Furthermore, a C-shaped nanoaperture or one of the related shapes is expected to provide ultrahigh light transmission (Shi *et al.*, 2003) with consequent high throughput. Our optical polarized nanosource basically consists of two separated metallic strips of a double C shape that are short-cut at the very end of the taper zone, that is, the end of the fibre near to the apex is fully coated as in a standard aperture fibre probe. This compound structure is able to drive a Quasi-TEM mode till about the apex. As a matter of fact, if the metal was perfectly conducting, a TEM mode would propagate in the structure. In the actual loss conductor case, the dominant guided mode becomes hybrid (HE) but still does not present a cut-off. Therefore, the propagation is not interdicted when the waveguide section becomes electrically (i.e. in terms of wavelength) small as normally occurs at probe tip. Probe performances are predicted by using CST Microwave Studio®, a commercial finite-difference time domain (FDTD)–based software. Results are compared with the case of an ordinary fully metal-coated tapered probe. The software automatically sets spatial meshing and time sampling to provide the desired accuracy. Following these simulations, we have manufactured and tested a probe prototype. The near-field light coming out from this probe is linearly polarized with an extinction ratio of 6 dB, as measured in the far field.

Materials and methods

The model

Polarization maintaining near-field optical probes can be treated by a classical electromagnetic model. The shape of common tapered aperture SNOM probes consists in a conical, metal-coated dielectric waveguide. The gradual decrease of the radius causes a progressive cut-off of the electromagnetic modes, and leads to a drastic attenuation of the optical power transmitted by the probe. A sketch of this probe is reported in Fig. 1a. In such a guide structure, the fundamental mode is the TE_{11}; the cut-off frequency f_{COTE11} is given by the first

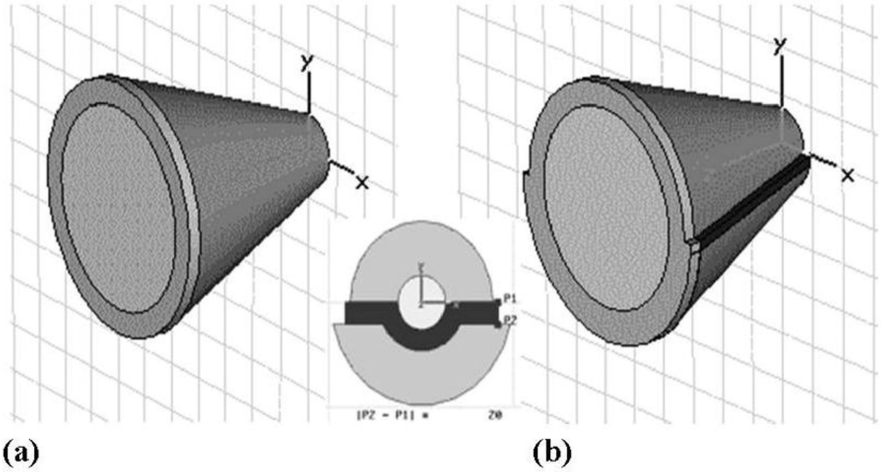

Fig. 1. Perspective of (a) an ordinary fully metal-coated tapered probe; (b) a tapered probe with a metal-coated Double C–shaped structure. The inset shows the transversal section at the apex of the (b) probe.

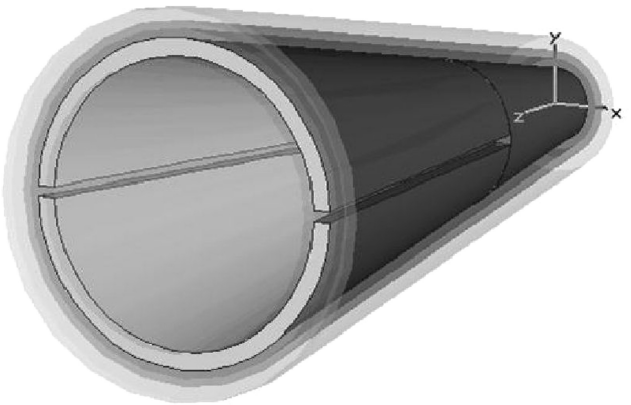

Fig. 2. Perspective of the Double C novel probe configuration, short cut at the end. The entire probe length is 2 μm; the short cut (fully metal-coated) is 600 nm.

zero in the first-order Bessel function derivative $J'_1(x)$(Balanis, 1989):

$$f_{\mathrm{COTE11}} = \frac{1,84 v_{\mathrm{p}}}{2\pi r},$$

where v_{p} is the phase velocity of the wave in the guide and r is the radius of the guide.

Such a limitation of near-field probes is related to the use of one-conductor waveguide structures, for example, a fully metal-coated taper (Hecht *et al.*, 2000). The problem can be overcome by using a two-conductor waveguide structure able to support a Quasi-TEM mode with no cut-off frequency. In this frame we have investigated two aperture probe configurations called Double C and Short-cut Double C, respectively (Figs 1b and 2). For both probe models, as well as for an *ordinary* metal-coated tapered probe (Fig. 1a), have been carried out an FDTD computation of the electromagnetic field distribution at the aperture. In particular, for the simulation has been considered a tapered fibre core with an angle of 20° and an apex radius of 50 nm. The simulation process has required the definition of the feeding port. It specifies the transition between the circular waveguide, where the fundamental TE_{11} mode is propagating, and the conical waveguide. At the same time it allows to set the polarization state of the light coupled to the tapered zone. The port was represented by the rings at the base of the cones (Figs 1 and 2). Furthermore, the dielectric core of the simulated structures is covered by different layers of material. As regards the standard probe, it has been considered an aluminium metal coating of 50 nm thickness (Fig. 1a). The taper zone of the Double C probe is coated with two metal slabs (aluminium layer of 50 nm thickness) separated with a dielectric spacer (LiF layer of 25 nm thickness) (Fig. 1b). Short-cut Double C is a little bit more complicated. It comprises an Al layer (thickness 50 nm) that realizes the Double C ending with a short conical waveguide. This first structure is covered with a 25-nm-thick dielectric layer (LiF) and a 25 nm + 25 nm thick Cr/Al layer (Fig. 2). The last three layers need to avoid the light leaking from the gap between the two C's. In fact, this field is present near the nanoaperture and it would seriously spoil the near-to-far field ratio. The dielectric/metal coating preserves the 'Short-cut Double C' structure while avoiding the lateral light leaking.

The probe

Following the model described earlier, we fabricated some Short-cut Double C probe prototypes. The adopted fabrication process is described in what follows. We start from a multi-mode–graded index optical fibre (model AFS50/12Y by Thorlabs Inc., Newton, NJ, USA) with a core diameter of 50 μm and a cladding of 125 μm. The bare tip is obtained by means of the tube etching method (Stöckle *et al.*, 1999). After the etching process, the probe is coated by thermal evaporation in ultra high vacuum. To realize the Shortcut Double C design, we first deposit two aluminium layers on the two opposite faces of the apex. To this purpose, we use a vacuum-compatible holder able to drive the rotation of the fibre along its axis. The holder consists of a steel cylinder coupled at one end to a stepper motor (1.8°/step). On the second end of the cylinder, a small channel accommodates the optical fibre exactly along its axis to realize a collinear structure. The stepper motor is driven from the outside of the vacuum chamber so that the entire process may be completed in a single run. The holder is mechanically connected to the chamber by means of a tilt movement. This additional mechanism is needed to optimize the position of the probe with respect to the crucibles. The first C is obtained by exposing one side of the fibre to the aluminium vapours. Subsequently, after a holder rotation of 180°, the opposite face is coated. In both cases we deposit a 50-nm thin metal layer. In Figs 3a and b are reported the SEM images of the probe after this fabrication stage. The magnification of the images allows to clearly visualize the formation of the Double C structure and the occurring of the short cut at few micrometres away from the taper apex (Fig. 3). Subsequently, a layer of 25 nm of LiF is deposited uniformly all around the taper region to insulate the Double C layer from the successive chromium and aluminium coating (50 nm). The probe so ultimate is analyzed by SEM (Fig. 4) in order to check the coating quality.

Results and discussion

The angular spectrum of the electric field (amplitude) is computed in the near field on a plane at $z = 25$ nm, that is, one spatial sample, away from the probe aperture. Figure 5 shows the results obtained simulating the standard full metal-coated aperture probe and the Double C aperture one. The scales on the x and y axes are the product of the spatial frequency [defined as $f_x = (2\Delta x)^{-1}$ and $f_y = (2\Delta y)^{-1}$] times the radiation wavelength. In this *reduced* system of coordinates, $x = |1|$ and $y = |1|$ are equal to $\lambda/2$; therefore, the sub-diffraction wavelength components lie outside the interval $(-1, +1)$. The

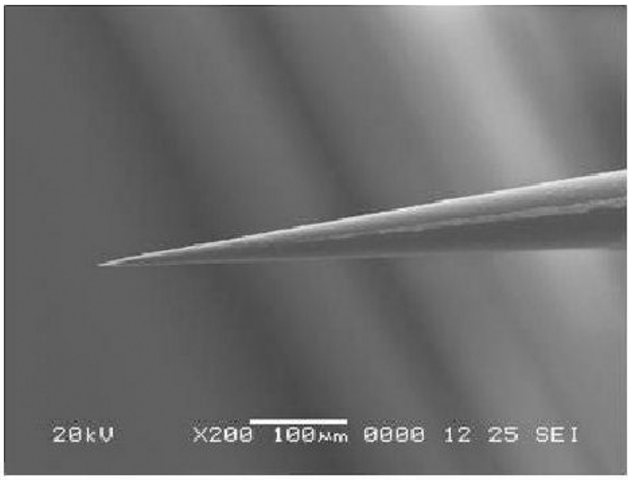

(a)

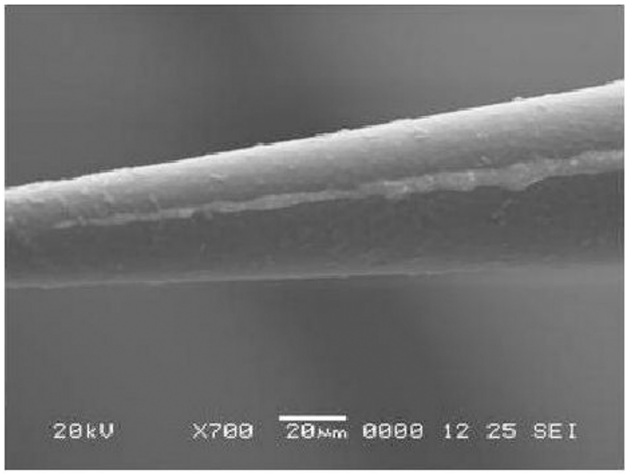

(b)

Fig. 3. (a) SEM image of the Short-cut Double C aperture probe prototype after the first aluminium deposition. It is visible that two separated strips of Al with a Double C shape have been formed. The lighter line is a zone of the fibre where no aluminium is present. (b) Magnification of the image (a) with a better-visible dielectric separation line and metal short-cutting.

probe is fed with a radiation polarized first along y and then along x. The output fields are calculated in both polarization directions y and x.

Figures 5a and d display the angular spectrum of the standard probe fed with the E_y component of the electric field. The spectra show an isotropic distribution of the E_y component (Fig. 5a) and a narrow spectrum of the E_x component (Fig. 5b), respectively. In particular, the E_x evanescent components have low amplitude. Because of the structure symmetry, the other spectrum component would show the same result in the opposite direction; therefore, here we report only the spectrum obtained feeding with one polarization direction. Clearly, these are the expected behaviours pointing

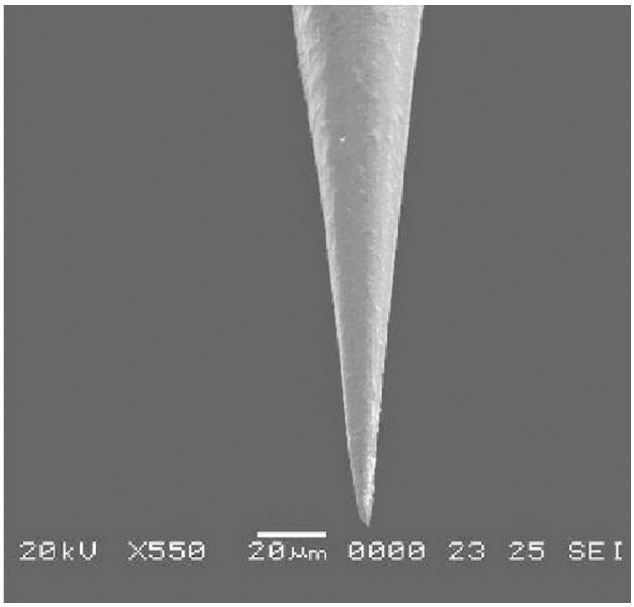

Fig. 4. SEM image of the Short-cut Double C prototype after, respectively, LiF and Al–Cr coatings.

out that the standard probe is not able to select a well-defined state of polarization.

The angular spectra obtained by feeding the Double C–shaped probe with E_y are reported in Figs 5b and e, which show the amplitude of the electromagnetic field components E_y an E_x in the x and y direction, respectively. Figs 5c and f report the amplitude spectrum of the components E_y and E_x, respectively, calculated feeding the structure by E_x. The propagating field has higher amplitude than the evanescent one, and the spectrum has two lobes with higher amplitude in the x direction, indicating a strong confinement of the aperture field in the x direction. The polarization of the evanescent field is mainly along the Double C y axis. The structure efficiently couples only the input E_y mode; as regards the evanescent zone, a very weak spectrum is observed in connection with an E_x feeding. Indeed, the spectrum reported on the Fig. 5e has on average lower amplitude. In particular, the evanescent components are almost negligible, and therefore the probe allows a low coupling in the direction crossed with respect to the y axis of the Double C structure. The four lobes of spatial frequencies placed in the propagating zone account for the possible components of the input E_y that are coupled with the edges of the Double C structure. The narrow distribution and the very low amplitude of the spectra reported in Figs 5c and f show that for input components of the electric field orthogonal to the Double C structure (x direction), the output is very low and the evanescent components are few. This simulation indicates that the Double C structure provides a general improvement on power magnitude of the overall angular spectrum and it is able to select a well-defined state of polarization. This behaviour is expected since a two-conductor

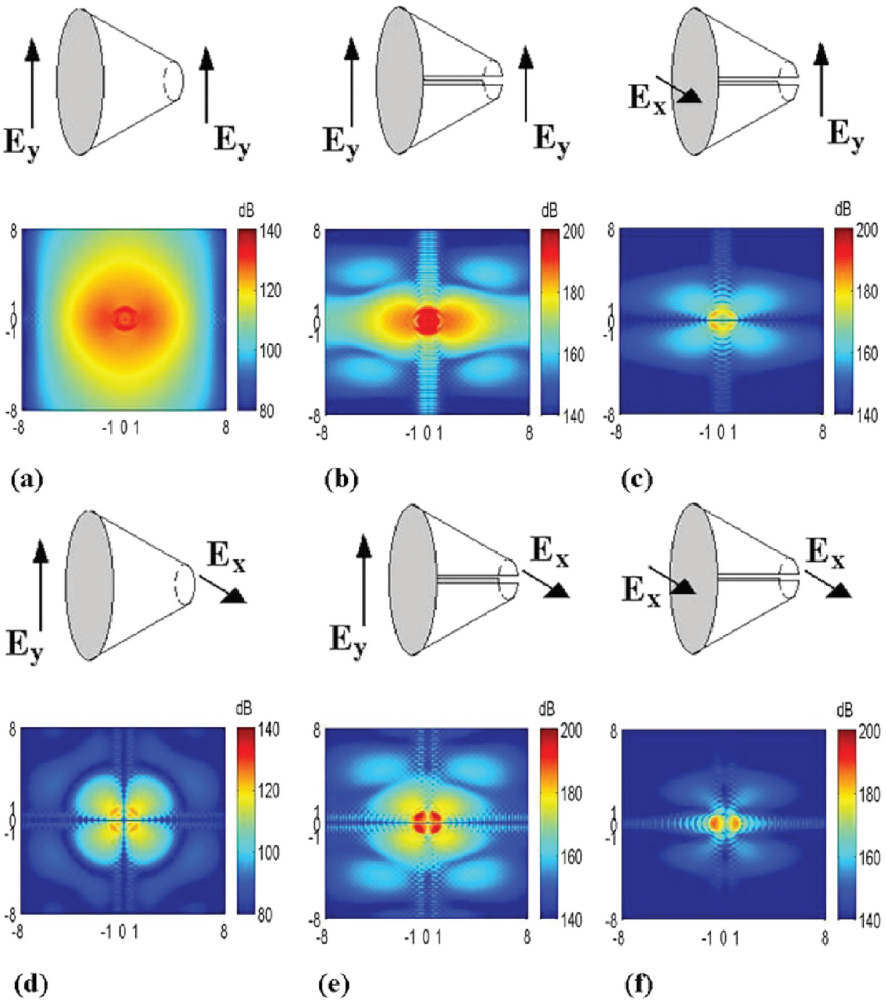

Fig. 5. Spectrum of electric field (in dB) on an xy plane at $z = 25$ nm away from the probe aperture, for both structures of Fig. 1. In the first column, the standard probe is fed with the E_y component of the field. In the second and third column, the Double C probe is fed with the E_y and E_x, respectively. The propagative components of the electric field are between -1 and 1, the remaining part accounts for the evanescent region of the spectrum.

structure drives a Quasi-TEM mode with no cut-off frequency till the end of the probe. However, it presents a drawback: the increased power lies in the propagating components, that is, the probe is not suitable for near-field microscopy.

The Short-cut Double C structure (Figs 2–4) overcomes this limit. By the present arrangement, the Quasi-TEM mode is driven very close to the end of the probe without cut-off. The polarization state is defined by the Double C topology, whereas the short conical waveguide attenuates the radiating part of the field, maintaining alive the evanescent components. Of course, the shorter is the cone, the higher is the near-field amplitude. The angular spectrum of the electric field amplitude of this new structure is presented in Fig. 6. The first row (Figs 6a and b) shows the E_y spectrum obtained by feeding the short-cut Double C structure with E_y and E_x, respectively. The second row (Figs 6c and d) displays the amplitude of the E_x components obtained by feeding the probe again with E_x and E_y. We can observe that, feeding the structure along the y and x axes of the structure, the spectra are pretty similar but one is attenuated with respect to the other. Such spectra are different from those calculated for the pure Double C. Indeed in this case, independently from the direction of the fed component of the electric field, the output spectra have the same distribution of spatial frequencies along y and x, respectively, corresponding to an aperture field well confined in both the dimensions. In particular, the spectra on Figs 6a and b have an isotropic distribution of components as for the standard probe. The spectra calculated in a direction orthogonal to the Double C structure (i.e. x) present much lower amplitude and a narrow distribution concentrated around the propagating zone. Thus, the ratio between the near-field and the far-field component is improved because most of the amplitude is distributed on the evanescent components (Figs 6a and b). Such result confirms that the Short-cut Double C probe acts as a polarizer producing

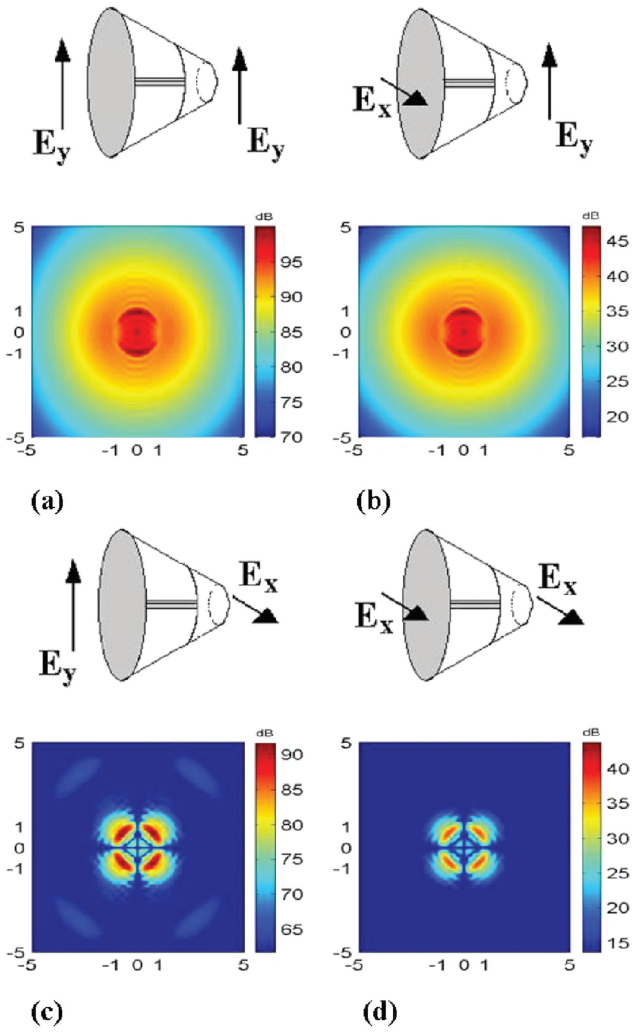

Fig. 6. Spectrum of electric field (in dB), on an *xy* plane at 25 nm from the probe aperture, for the Short-cut Double C structure of Fig. 2. On the first [second] row, the calculated E_y [E_x] component are shown. In the first and second column, the Double C probe is fed with the E_y and E_x, respectively. The radiative region of the electric field is between −1 and 1, the remaining part accounts for the evanescent region of the spectrum.

a near-field light linearly polarized regardless the polarization state of the light coupled into the fibre.

To characterize in far field the polarizing properties of the Short-cut Double C SNOM aperture probe, we couple to the fibre the unpolarized light emitted by an LED at 538 nm. In front of the SNOM probe aperture is placed a focussing objective (50×, NA 0.52) and a rotating holder carrying a linear polarizer. The LED current is modulated by the reference signal coming from a digital lock-in and the light emitted by the probe is detected in phase by a photomultiplier. The results of the optical intensity versus the polarizer angle are reported in the polar diagram shown in Fig. 7. The distribution of the light along the polarizer angle indicates that the light coming out from the SNOM is almost linearly polarized with an

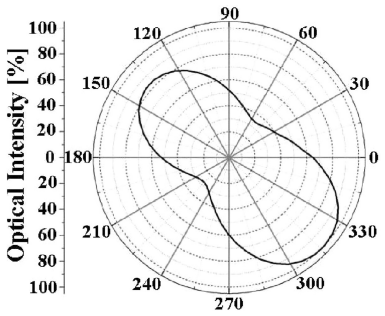

Fig. 7. Polar diagram of the Short-cut Double C probe prototype. The shape of the diagram indicates that the light coming out from the probe is linearly polarized, with an extinction ratio of 6 dB.

extinction ratio of 6 dB. Such a result shows that the prototype probe is able to produce a near-field light with a well-defined polarization state as predicted by the FDTD model. The slight asymmetry observed in the polar diagram could be ascribed to small grain imperfections on the metal coating of the aperture. Furthermore, better near-field polarization ratios are expected when the source coupled to the fibre is a polarized one. This is the common situation in an SNOM experiment where usually a polarized laser beam is coupled to the probe.

It is worth mentioning here that the short-cut Double C structure closely resembles the hollow-pyramid cantilevered near-field probes (HPC) (Mihalcea *et al.*, 1996). They consist of hollow metal-coated aperture tips integrated in a conventional force cantilever and are known to maintain the polarization (Oesterschulze *et al.*, 1998) because they are very short. Recently, this important property was confirmed by a direct characterization in near field (Biagioni *et al.*, 2005). Although HPC probes cannot produce a well-defined polarization state from unpolarized light, when they are fed by a defined polarized field coming from a laser source they maintain the polarization of the incoming light. In this case, they operate like our Short-cut Double C structure.

Conclusions

This work reports about modelling and realization of a novel aperture SNOM probe able to select a well-defined polarization state named Short-cut Double C probe. It consists of a two-conductor conical waveguide structure that blends, at the apex, into a small single-conductor waveguide. Numerical FDTD simulations were performed in order to evaluate the angular spectrum of the electric field amplitude at the nanometric probe aperture. Such calculations show that the near-field spectrum is qualitative independent of the polarization state of the incoming light and that the electromagnetic field emerging from the probe aperture has a well-defined polarization. Following the parameters given by the simulation, we have fabricated a probe prototype. Far-field polarization measurements of the near field coming out from

this novel aperture probe confirm the predicted polarization behaviour.

References

Adelmann, C., Hetzler, J., Scheiber, G., Schimmel, Th., Wegener, M., Weber, B. & Lohneysen, H.V. (1999) Experiments on the depolarization near-field scanning optical microscope. *Appl. Phys. Lett.* **74**, 179–181.

Adiga, V.P., Kolb, P.W., Evans, G.T., Cubillos-Moraga, M.A., Schmadel, D.C., Dyott, R. & Drew, H.D. (2006) Development of high-throughput, polarization-maintaining, near-field probes. *Appl. Opt.* **45**, 2597–2600.

Ambrosio, A., Alderighi, M., Labardi, M., Pardi, L., Fuso, F. & Allegrini, M. (2004) Near-field optical microscopy of polymer-based films with dispersed terthiophene chromophores for polarizer applications. *Nanotechnology* **15**, S270–S275.

Balanis, C.A. (1989) *Advanced Engineering Electromagnetics.* Wiley, New York.

Betzig, E., Trautman, J.K., Weiner, J.S., Harris, T.D. & Wolfe, R. (1992) Polarization contrast in near-field scanning optical microscopy. *Appl. Opt.* **31**, 4563–4568.

Biagioni, P., Polli, D., Labardi, *et al.* (2005) Unexpected polarization behavior at the aperture of hollow-pyramid near-field probes. *Appl. Phys. Lett.* **87**, 223112-1-3. Erratum *Appl. Phys. Lett.* **88**, 209901.

Fasolka, M.J., Goldner, L.S., Hwang, J., Urbasm, A.M., De Rege, P., Swager, T. & Thomas, E.L. (2003) Measuring local optical properties: near-field polarimetry of photonic block copolymer morphology. *Phys. Rev. Lett.* **90**, 016107-1-4.

Hecht, B., Sick, B., Wild, U.P., Deckert, V., Zenobi, R., Martin, O.J.F. & Pohl, D.W. (2000) Scanning near-field optical microscopy with aperture probes: fundamentals and applications. *J. Chem. Phys.* **112**, 7761–7774. And references therein.

Huser, Th., Novotny, L., Lacoste, Th., Eckert, R. & Heinzelmannm, H. (1999) Observation and analysis of near-field optical diffraction. *J. Opt. Soc. Am. A* **16**, 141–148.

Lacoste, T., Huser, T., Prioli, R & Heinzelmann, H. (1998) Contrast enhancement using polarization-modulation scanning near-field optical microscopy (PM-SNOM). *Ultramicroscopy* **71**, 333–340.

Lapchuk, A.S. & Kryuchyn, A.A. (2004) Near-field optical microscope working on TEM wave. *Ultramicroscopy* **99**, 143–157.

Lewis, A., Isaacson, M., Harootunian, A. & Murray, A. (1984) Development of a 500 Åspatial resolution light microscope *Ultramicroscopy* **13**, 227–231.

Likodimos, V., Labardi, M., Pardi, L., Allegrini, M., Giordano, M., Arena, A. & Patanè, S. (2003) Optical nanowriting on azobenzene side-chain polymethacrylate thin films by near-field optical microscopy. *Appl. Phys. Lett.* **82**, 3313–3315.

Mihalcea, C., Scholz, W., Werner, S., Münster, S., Oesterschulze, E. & Kassing, R. (1996) Multipurpose sensor tips for scanning near-field microscopy. *Appl. Phys. Lett.* **68**, 3531–3533.

Novotny, L. & Hafner, C. (1994) Light propagation in a cylindrical waveguide with a complex, metallic, dielectric function. *Phys. Rev. E* **50**, 4094–4106.

Novotny, L. & Hecht, B. (2006) *Principles of Nano-optics*. Cambridge University Press, Cambridge.

Novotny, L., Pohl, D.W. & Regli, P. (1994) Light propagation through nanometer-sized structures: the two-dimensional-aperture scanning near-field optical microscope. *J. Opt. Soc. Am. A* **11**, 1768–1779.

Oesterschulze, E., Rudow, O., Mihalcea, C., Scholz, W. & Werner, S. (1998) Cantilever probes for SNOM applications with single and double aperture tips. *Ultramicroscopy* **71**, 85–92.

Ono, M., Sone, H. & Hosaka, S. (2005) Prototype of atomic force cantilevered SNOM based on through-the-lens-type optical lever and polarized illumination and detection system. *Jpn. J. Appl. Phys.* **44**, 5434–5437.

Pilevar, S., Edinger, K., Atia, W., Smolyaninov, I. & Davis, C. (1998) Focused ion-beam fabrication of fiber probes with well-defined apertures for use in near-field scanning optical microscopy. *Appl. Phys. Lett.* **72**, 3133–3135.

Pohl, D.W., Denk, W. & Lanz, M. (1984) Optical stethoscopy: image recording with resolution $\lambda/20$. *Appl. Phys. Lett.* **44**, 651–653.

Ramoino, L., Labardi, M., Maghelli, N., Pardi, L., Allegrini, M. & Patanè (2002) Near-field polarization detection and control for quantitative local dichroism mapping. *Rev. Sci. Instr.* **73**, 2051–2056.

Setälä, T., Kaivola, M. & Friberg, A.T. (2002a) Degree of polarization in near fields of thermal sources: effects of surface waves. *Phys. Rev. Lett.* **88**, 123902-1-4.

Setälä, T., Shevchenko, A. & Kaivola, M. (2002b) Degree of polarization for optical near fields. *Phys. Rev. A* **66**, 016616-1-7.

Shi, X., Hesselink, L. & Thornton, R.L. (2003) Ultrahigh light transmission through C-shaped nanoaperture. *Opt. Lett.* **28**, 1320–1322.

Shin, D.J., Chavez-Pirson, A. & Lee, Y.H. (1999) Diffraction of circularly polarized light from near-field optical probes. *J. Microsc.* **194**, 353–359.

Stöckle, R., Fokas, C., Deckert, V., Zenobi, R., Sick, B., Hecht, B. & Wild, U.P. (1999) High-quality near-field optical probes by tube etching. *Appl. Phys. Lett.* **75**, 160–162.

Valaskovic, G.A., Holton, M. & Morrison, G.H. (1995) Image contrast of dielectric specimens in transmission mode near field scanning optical microscopy: imaging properties and tip artifacts. *J. Microsc.* **179**, 29–54.

Veerman, J.A., Garcia-Parajo, M.F., Kuipers, L & VanHulst, N.F. (1999) Single molecule mapping of the optical field distribution of probes for near-field microscopy. *J. Microsc.* **194**, 477–482.

Veerman, J.A., Otter, A.M., Kuipers, L. & van Hulst, N.F. (1998) High definition aperture probes for near-field optical microscopy fabricated by focused ion beam milling. *Appl. Phys. Lett.* **72**, 3115–3117.

